

 <p>GKSS FORSCHUNGSZENTRUM in der HELMHOLTZ-GEMEINSCHAFT</p>	<p>MERIS Case2 Regional</p>	<p>ATBD water Page 1 of 19</p>
---	------------------------------------	------------------------------------

Algorithm Theoretical Basis Document (ATBD)

MERIS

Advanced Water Algorithm

Version 1.1, November 2006

Roland Doerffer & Helmut Schiller
GKSS Forschungszentrum Geesthacht GmbH
21502 Geesthacht

ESRIN Contract: No. 18639/04/I-LG
MERIS Case 2 Water Algorithms Development

Copyright © 2006 GKSS GmbH

Distribution

Name:

P. Regner (ESA / ESRIN)

C. Brockmann (Brockmann Consult)

Change Record

<u>Issue</u>	<u>Revision</u>	<u>Date</u>	<u>Description</u>
Draft 0.1	0	30.11.2005	Initial draft
Draft 0.2	1	23.12.2005	Updated draft
Version 1.1	2	24.11.2006	Final Version

Abstract	4
Design of the Procedure	4
Enhancement of the retrieval	6
Special feature: cut off reflectance	8
The bio-optical model	8
Pure water	10
Absorption by phytoplankton pigments	10
Absorption by yellow substance	11
Absorption by bleached particles	11
Scattering by all particles	11
Range and Co-variations	12
Environmental Conditions	13
Conversion from IOP to concentrations	13
Calculation of the minimum irradiance attenuation coefficient k_{\min} and the signal depth z_{90}	16
Validation of the algorithm enhancement	17
References	18

Abstract

The paper describes the case 2 coastal water algorithm, which is a further development of the ground processor of the Medium Resolution Imaging Spectrometer (MERIS). The enhancement consists in the replacement of the simple quality check by an optimization procedure improving the quality of the retrieval.

The algorithm derives the inherent optical properties (IOP) (1) absorption coefficient of phytoplankton pigment, (2) absorption coefficient of *gelbstoff* and total suspended matter after bleaching the phytoplankton pigment fraction and (3) the scattering coefficient of total suspended matter (TSM). The IOPs of (1) and (3) are converted also into the concentrations of chlorophyll a and TSM dry weight. The algorithm is based on a neural network (NN), which relates the bi-directional water leaving radiance reflectances with these IOPs. The network is trained with simulated reflectances. The bio-optical model used for the simulations is based on a large data set collected mainly in European waters.

The algorithm is based on Neural Net (NN) technology. Two NN's are trained with simulated reflectances:

1. *invNN* to emulate the inverse model
(reflectances, geometry) \rightarrow concentrations, and
2. *forwNN* to emulate the forward model
(concentrations, geometry) \rightarrow reflectances.

The *invNN* is used to obtain an estimate of the concentrations which is used as a first guess to start a minimization procedure, which uses the *forwNN* iteratively to minimize the difference between the calculated reflectances and the measured ones. The procedure is fast as it takes advantage of the Jacobian which is a byproduct of the NN calculation.

Design of the Procedure

The NN, which is used in the ground-segment of MERIS, transforms directional water leaving radiance reflectances measured in eight spectral bands (outcome of the atmospheric correction procedure of the MERIS ground segment) and the three angles pixel by pixel with high efficiency into three inherent optical properties, i.e. (1) scattering of all particles b_{tsm} , (2)

absorption of phytoplankton pigments a_{pig} and (3) absorption of gelbstoff + the bleached fraction of suspended matter a_{gelb} . The IOPs b_{tsm} and a_{pig} are then converted by simple equations into concentrations of the water constituents suspended matter and phytoplankton, while *gelbstoff* remains in absorption units. This separation has the advantage that the IOPs can also be used directly or converted into concentrations by other coefficients determined by the user.

The directional water leaving radiance reflectance $RL_w(\theta_v, \phi_v)$ associated with the water leaving radiance $L_w(\theta, \phi)$ and the downwelling irradiance above the sea surface E_d is defined to be:

$$RL_w(\theta_v, \phi_v) = L_w(\theta_v, \phi_v) / E_d(\theta_s)$$

where θ_v and ϕ_v are the zenith and azimuth observation angles respectively. E_d depends on the solar zenith angle, θ_s , for the pixel under examination. For convenience we will denote the wavelength dependency in the following chapters only where necessary.

Since simultaneous measurements of concentrations and water leaving radiance reflectance spectra are rare and, thus, do not cover the data space with sufficient density, the construction of the NN is based on a large table (550K entries) of simulated data generated by our forward model which was built from the *HYDROLIGHT* radiative transfer code (Mobley 1994) plus a bio-optical model relating scattering and absorption coefficients to concentrations.

This bio-optical model is based on a large data set of measurements of inherent optical properties and describes the variability of the three major components of coastal waters, i.e. scattering by all particles, absorption by phytoplankton pigments and absorption by humic organic matter (*gelbstoff*). The optical data are mainly from cruises in the North Sea, partly in the Baltic Sea, Mediterranean Sea and North Atlantic.

For given concentrations / IOPs of water constituents the forward model calculates the angular distribution of water leaving radiance in eight visible MERIS bands. These angular distributions are sampled in the appropriate angle ranges to derive the entries of the training / test tables for building the NN: three concentrations, three angles and eight water leaving radiance reflectances. The concentrations of the water constituents are randomly sampled from an exponential distribution in order to disentangle small concentration differences in regions of small concentrations. In order to get roughly constant relative concentration errors the logarithm of the IOP's was used as NN output.

To avoid extrapolation from the training set the NN has to learn the variability of the inherent optical properties (IOP) of the water constituents as well as the errors in reflectances caused by the instrument and the atmospheric correction. Thus, the natural variability of the IOPs was built into the forward model by sampling the parameters describing the spectral dependence of the IOPs from their measured distributions

Two NN's are trained (Schiller, 2000) with this table: (1) *invNN* to emulate the inverse model $\mathbf{c} = F_g^{-1}(\mathbf{r})$ from reflectances \mathbf{r} and geometry information g , and (2) *forwNN* to emulate the forward model $\mathbf{r} = F_g(\mathbf{c})$ deriving reflectances \mathbf{r} from concentrations \mathbf{c} and geometry information g .

In the MERIS ground segment (Schiller and Doerffer, 1999) the two NN's are combined to give a new NN (s. Fig. 1), which first uses the *invNN* part to obtain an estimate of the concentrations \mathbf{c} . These together with the geometry information \mathbf{g} are fed into the *forwNN*. If not only the measurement of the reflectances but also the model is perfect the identity $\mathbf{r} = \mathbf{F}_g(\mathbf{F}_g^{-1}(\mathbf{r}))$ should hold. Therefore the reflectances \mathbf{r}' returned by the *forwNN* are compared with the measured ones. Large deviations signal a violation of the necessary condition for a successful inversion; corresponding pixels are then flagged (Doerffer and Schiller, 2000)).

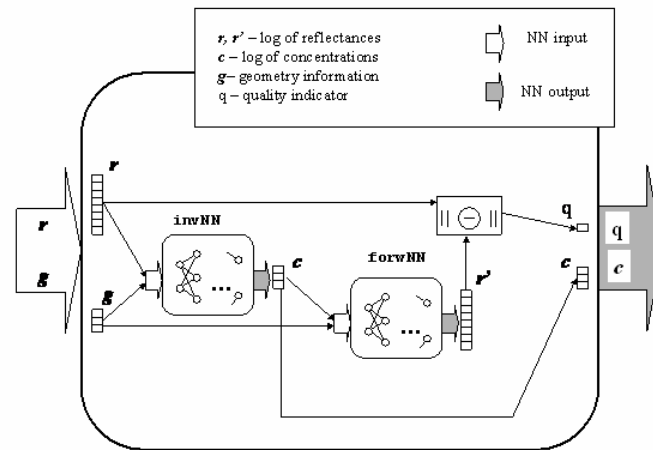


Fig. 1 A combination of NN's is used in the MERIS ground segment for the retrieval of water constituent concentrations \mathbf{c} from remotely sensed reflectances \mathbf{r} and geometry information \mathbf{g} . The \mathbf{c} obtained from the *invNN* emulating the inverse model is used together with the geometry information \mathbf{g} as input to the *forwNN* which calculates the corresponding reflectances \mathbf{r}' which are compared with the measured ones to give a quality measure q of the retrieval.

Enhancement of the retrieval

The advanced algorithm (Schiller and Doerffer, 2005) is depicted in fig. 2. Now after the comparison of the reflectances \mathbf{r}' returned by the *forwNN* with the measured ones optimization steps are inserted. The aim is to improve the agreement of \mathbf{C} with \mathbf{r} by iteratively adjusting the estimate \mathbf{c} .

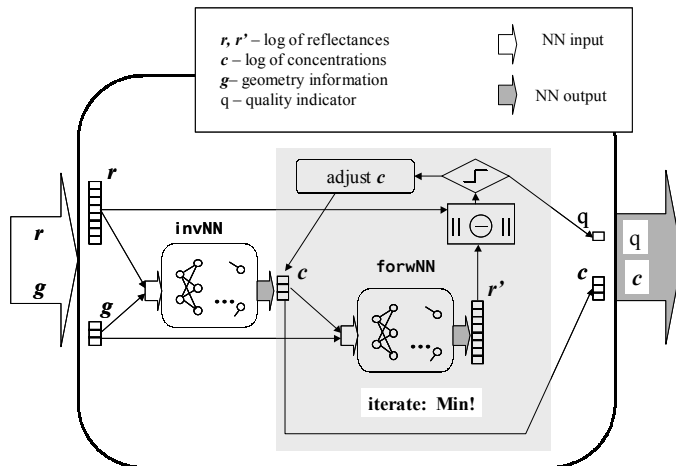


Fig. 2 In the enhanced algorithm the optimization loop replaces the simple quality check.

We apply the Levenberg-Marquardt minimization algorithm which reads for our problem like follows:


The error sum to be minimized is $(\mathbf{r}' - \mathbf{r})^2 / 2$. We have an estimation of \mathbf{c} . Application of the NN not only allows to get $\mathbf{r}' = \text{forwNN}(\mathbf{c})$ but also to calculate the Jacobi matrix $\mathbf{Z}_{ni} = \frac{\partial r'_n}{\partial c_i}$.

The new estimate is $\mathbf{c}_{new} = \mathbf{c}_{old} - (\mathbf{Z}^T \mathbf{Z} + \lambda \mathbf{I})^{-1} \mathbf{Z}^T (\mathbf{r}'(\mathbf{c}_{old}) - \mathbf{r})$. If the resulting error is less than the old one the new estimate is accepted and the next iteration step is done with

$\lambda \leftarrow \lambda / 20$. Otherwise the trial is repeated with $\lambda \leftarrow \lambda \times 20$. (At the very beginning $\lambda = 0.01$). We stop the optimization loop after at most 10 iterations or if the relative error change is less than 3% or if all parameters change < 0.005 .

In summary the algorithm development consists of the following steps:

- Set up of a bio-optical model based on measurements of IOPs and concentrations including the natural variability of IOPs
- Definition of the range of concentrations and further boundary conditions (s. bio-optical model)
- Estimation of expected errors of RLW's based on instrumental errors and uncertainties of atmospheric correction
- Simulation of RLW spectra
- Training of the NN's
- Test of the NN's
- Use of the NN's within the processor
- Validation of the algorithm and the products

	MERIS Case2 Regional	ATBD water Page 8 of 19
--	-----------------------------	----------------------------

Special feature: cut off reflectance

A special features is the cut-off reflectance. The RLw, which are retrieved from the top of atmosphere radiances by the atmospheric correction procedure can be significantly inaccurate or even negative at low reflectances, e.g. in the red part of the spectrum in case 1 waters due to the high absorption of pure water or in the blue part in case of high concentrations of yellow substances. Since we use the logarithm of the reflectances even small absolute errors of these bands can degrade the performance of the NN significantly. In order to cope with such faulty input the NN was trained in such a way that the reflectance was set to $\log(\text{RLw})$ of -6.9 sr^{-1} whenever the reflectance is below this minimum. Accordingly the measured reflectances after atmospheric correction were treated in the same way. However a minimum of 3 bands with reflectances above this threshold is required to run the NN algorithm. This cut off feature improved the results significantly, because low reflectances data with a relative high noise or negative reflectances are excluded.

The bio-optical model

Water constituents comprise a large number of different substances, which include mineralic dissolved and particulate compounds, a large variety of organic macromolecules, living organisms such as phytoplankton, zooplankton, bacteria etc., and their debris and excrements. All of these water constituents have different optical properties concerning scattering and absorption and partly fluorescence.

For the purpose of optical remote sensing this diversity of substances has to be grouped into a small number of classes each of which includes constituents with similar optical properties and / or correlated concentrations. For the majority of the world ocean areas it is sufficient to comprise all substances into one group using phytoplankton chlorophyll *a* as a proxy for its concentration. This type of water is called case I water. The concentration of this class of substances - in terms of chlorophyll *a* - can be derived from the blue to green shift of the water colour. In many coastal waters one needs more than one class of substances to describe the variability of water colour. By tradition and experience three classes are defined: (1) phytoplankton pigment with chlorophyll *a* as a proxy, (2) the dry weight of all particles (total suspended matter, TSM) and (3) the absorption caused by the "dissolved" fraction of all water constituents (*gelbstoff*).

However, each of the three groups of substances is variable with respect to their composition and thus their chemical, physical and in particular optical properties. Any remote sensing system and retrieval algorithm has to take this variability into account.

Due to this fact it was decided for MERIS not to relate the output of the NN algorithm to the concentrations of these groups of substances but to three IOPs, which can be related to these substances,

Due to the restrictions of the MERIS processor, only three components could be defined, although others are possible. These are (1) phytoplankton pigment absorption *a_{pig}*, (2) absorption of all other substances *a_{gbp}* (dissolved *gelbstoff* *a_{gelb}* and bleached particulate matter *a_{bp}*) and (3) scattering of all particles *b_{tsm}* with the assumption that the scattering

component is not absorbing, i.e. that the absorption, which modifies the volume scattering of absorbing particles, is covered by the absorption a_{pig} and a_{bp} . All three optical components are defined for the wavelength of MERIS band 2 (442 nm). Furthermore, the optical component b_{tsm} is represented by two types of scattering particles. One is a standard particle with a wavelength exponent of 0.4 and another white scatterer with a wavelength exponent of 0.0. This white scatterer was introduced to get a representation for coccolithophorides.

An overview of all components with their properties is given in table 1.

The components are defined according to the separation and measurement procedures (Fig. 3). One critical issue is the separation of the absorption of phytoplankton pigments and the absorption of other substances, which are part of suspended matter. This separation is performed by oxydation of the TSM using NaHCl. The difference in the absorption spectrum before and after this treatment is assumed to be the absorption of all phytoplankton pigments. Another issue is the separation between dissolved yellow substance and the absorption of TSM, which is determined by the type and pore size of the filter used for separation, which traditionally was 0.45 μm and nowadays is 0.2 μm .

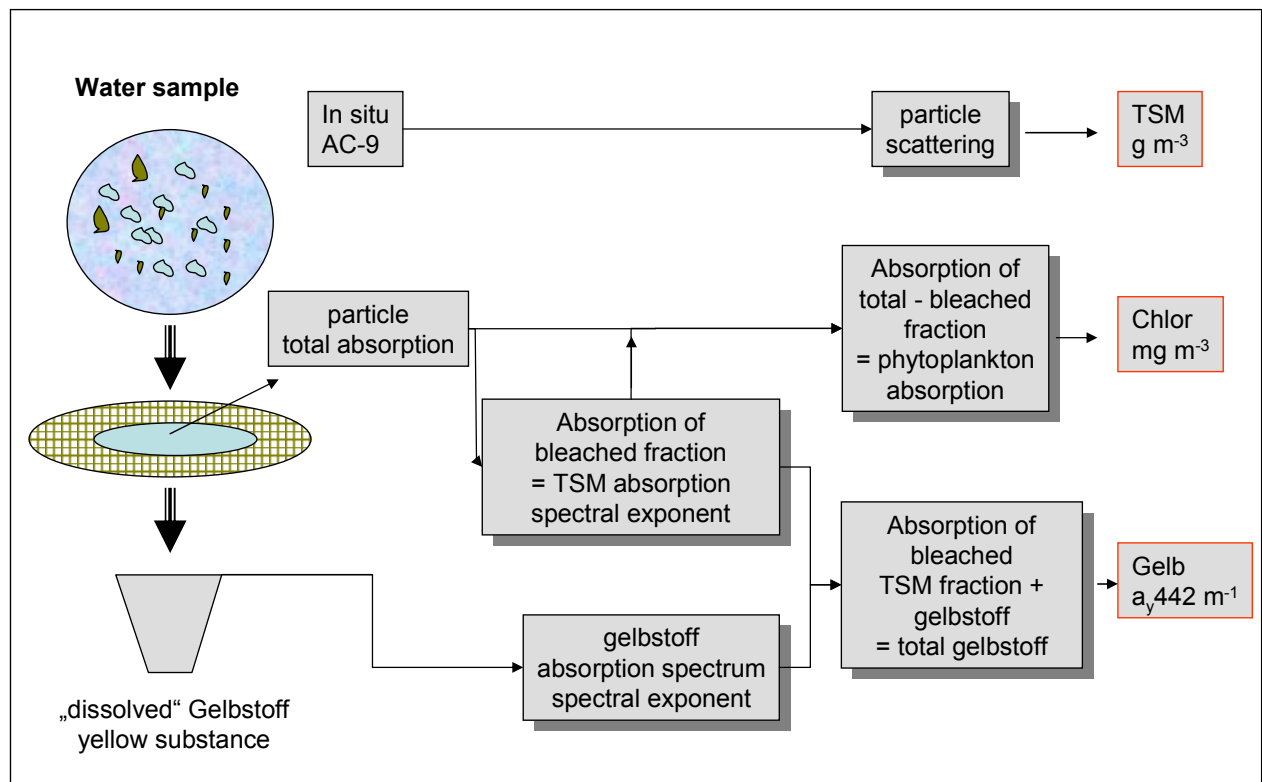


Fig. 3 Scheme of the bio-optical model: The water sample is divided by filtration into a “dissolved” fraction and particulate fraction. The particulate fraction is bleached. The difference between the total particulate absorption and the absorption after bleaching is defined as the phytoplankton pigment absorption. Its value at 442 nm is a_{pig} . The absorption of the bleached fraction is added to the absorption of the “dissolved” fraction and provides the gelbstoff absorption at 442 nm. The scattering component is measured with the AC-9 instrument. It provides the total scattering of all particles at 442 nm.

The quantitative relationship between the concentration of a bio-geochemical component and its optical proxy is described by a conversion factor or equation, which - for MERIS - can be adapted to local conditions or exchanged by the user based on his experience.

Phytoplankton pigment absorption a_{pig} is related to chlorophyll *a* concentration (in $\mu\text{g/l}$), the scattering of non absorbing particles b_{tsm} is related to the dry weight of total suspended matter (TSM, in mg/l) and the sum of the absorption of gelbstoff a_{gelb} and of the bleached particulate matter, a_{bp} , is related to the *gelbstoff* absorption a_{gelb} (in $1/\text{m}$). The mean conversion factors and equations are based on the results of the projects COASTLOOC and COLORS/MAPP, REVAMP, MAVT, for details s. below.

All measurements of optical properties have been carried out according to the protocols set up by ESA MAVT, which in turn is based on the protocols set up for the COLORS project and the SeaWiFS project.

Pure water

The absorption of pure water is based on the measurements of Pope and Fry (1997), the scattering of pure water on the formulation of Morel (1974).

Absorption by phytoplankton pigments

The variability of phytoplankton pigments is represented by a series of 221 spectra (Fig. 4) of which one is selected randomly for each simulation of the reflectance spectrum. This set of spectra has been compiled from measurements in the Southern North, in the Skagerrak and the North Sea off Norway in the period 2000 - 2003. All measurements have been performed according to the same protocol using the filter pad method (s. Soerensen, this volume).

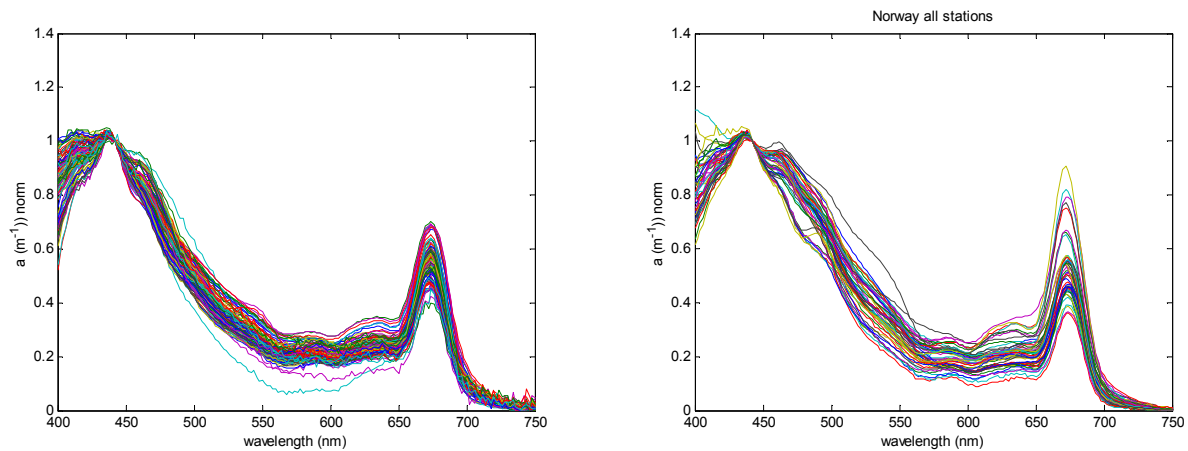


Fig. 4 Absorption spectra of phytoplankton pigments (difference between non bleached and bleached fraction of total suspended matter), normalized at 442 nm, i.e. for MERIS spectral band 2. The left panel shows spectra of the Southern North Sea. The right panel shows spectra of Norwegian coastal waters including the Skagerrak (courtesy of K. Soerensen, NIVA, Norway).

Absorption by yellow substance

Yellow substance a_{gelb} is defined here as the absorption at 442 nm of all water constituents which pass a Millipore filter with a pore size of 0.2 μm . The wavelength exponent of the quasi exponential decrease of absorption with increasing wavelength was determined from the wavelength range 400 – 550 nm using a non-linear fit method. No offset subtraction at 750 nm was performed. To determine the mean and standard deviation of the wavelength exponent, measurements were compiled from the Southern North Sea, the Skagerrak and the coastal waters of western Norway.

Absorption by bleached particles

Particles are defined as all substances, which remain on a glassfibre filter (Type Whatman GFF,) after filtration. The absorption properties are determined after deterioration of the phytoplankton pigments using NaHCl. These absorption spectra look very similar to those of yellow substance but with a lower wavelength exponent. This exponent was determined in the same way as that of yellow substance.

Scattering by all particles

The total volume scattering b [m^{-1}] of all particles has been measured in situ at 9 wavelength with an AC-9 instrument, which determines absorption and beam attenuation. This instrument was attached together with other instruments to a rosette water sampling frame, so that water samples could be taken simultaneously with the measurement. The spectral exponent was then determined from all wavelengths using a non linear fit. Furthermore, the results were checked against data of the COASTLOOC project (Babin 2003), which covered coastal and off shore areas of the Mediterranean, the Atlantic, North and Baltic Sea, and compared to results of Siegel et al. (2005) for the Baltic area.

In addition a white scatterer (spectral exponent of 0) was introduced to include the effects of coccolithophorides, which often occurs in the North Sea and Keltic Sea during summer months. However, due to the restrictions of the MERIS products format, the white scatterer is not a separate variable, only the optical effect was introduced so that the NN learned that this kind of material may be present in the water.

The scattering phase function of Petzold as described in (Mobley 1994, table 3.10) was used for standard TSM and white particles.

The concentrations of all particles are determined as the dry weight per volume of water.

Range and Co-variations

According to the data from North Sea Water and the concentration ranges in case 1 water (ATBD Morel and Antoine 2000) the range for pigment and gelbstoff absorption (a_{pig} and a_{gelb}) as well as particle and white particle scattering b_{tsm} (442 nm) was set as listed in table 1.

Although all variables should vary as independently as possible within the given ranges, we have introduced some restrictions concerning the minimum scattering associated with the absorption coefficients of phytoplankton pigments and bleached particles in order not produce unrealistic low reflectances.

These minima were determined from the covariations between absorption and scattering.

The following relationships were determined:

$$b_{tsm_min} = 0.25 * a_{pig}(442nm)$$

The co-variation between the absorption coefficient of bleached particles and the scattering coefficient of total suspended matter scattering was determined as:

$$a_{tsm_bleached}(442\text{ nm}) = 0.1 * b_{tsm}(442) + ran_gauss * 0.03 * b_{tsm}(442)$$

where ran_gauss is a random number of a $N(0,1)$ Gaussian probability distribution.

Note that the coupling excludes some extreme combinations, which however might occur in nature.

<i>Component / property</i>	<i>value range</i>
Gelbstoff absorption wavelength exponent	0.014 +- 0.002
Bleached particle absorption wavelength exponent	0.008 +- 0.005
Particle scattering wavelength exponent	0.4 +- 0.2
White particle scattering wavelength exponent	0.0

<i>Component / property</i>	<i>value range</i>
Phytoplankton pigment absorption	random selection from > 200 absorption spectra, normalized at 442 nm (MERIS band 2)
Gelbstoff absorption a_gelb at 442 nm	0.005 - 5.0 m-1
Particle scattering bp at 442 nm	0.005 - 30.0 m-1
White particle scattering bpw at 442 nm	0.005 - 30.0 m-1
Phytoplankton pigment absorption a_pig at 442 nm	0.001 - 2.0 m-1
Minimum particle scattering at 442 nm	$0.25 * a_pig(442nm)$
Bleached particle absorption	$0.1 * bp(442) + ran_gauss * 0.03 * bp(442)$
Sun zenith angle	0 - 80 degree
Viewing zenith angle	0 - 50 degree
Difference between sun and viewing azimuth angle	0 - 180 degree

Table 1: Variability of the optical properties and range used for the simulation of water leaving radiance reflectance spectra

Environmental Conditions

The environment as well as further optical properties were defined in the following way: infinite deep water (no bottom effect), vertical homogenous distribution of all water constituents, rough sea surface according to a wind speed of 3 ms^{-1} .

The downwelling radiance distribution above water has been simulated with Hydrolight, which was adapted for this purpose to simulate an atmosphere with 50 layers for 17 solar zenith angels ranging from 0 to 80 degree.

Furthermore no inelastic scattering (fluorescence or Raman scattering) as well as no polarisation effects have been considered in the simulation.

Conversion from IOP to concentrations

Although the primary output of the NN algorithm are the logarithms of the three IOPs, i. e. phytoplankton pigment absorption, gelbstoff + bleached particle absorption and total suspended matter scattering, it was decided by ESA to convert the scattering coefficient into total suspended matter dry weight concentration in mg/l and the phytoplankton pigment

absorption into chlorophyll *a* concentration. However, this conversion should be reversible to enable a user to go back to the IOPs from the concentrations and then may apply his own conversion factors. Thus, only single relationships between one IOP and one concentration were allowed. As for the optical properties, these relationships can be rather variable with respect to geographical regions and seasons and no global data base exists concerning coastal waters. Thus, we have based the correlations on our own measurements in the North Sea and compared the results with data of Norwegian waters provided by K. Soerensen. Furthermore, we compared the pigment absorption with the chlorophyll *a* concentrations, as derived with the case 1 water algorithm of MERIS (algal_1 product, Morel & Antoine). This reflectance ratio algorithm is based on a nearly global open ocean data set and has been developed totally independent from the algal_2 neural network algorithm. However, these comparisons are indicators; a significance test in a strict statistical sense could not be performed, because the properties of the data sets are too different.

Based on the data set of our cruises in the Southern North Sea we found the following relationship for phytoplankton pigments:

$$\text{chl. conc } [\mu\text{g/l}] = 21 * a_{\text{pig}}^{1.04}$$

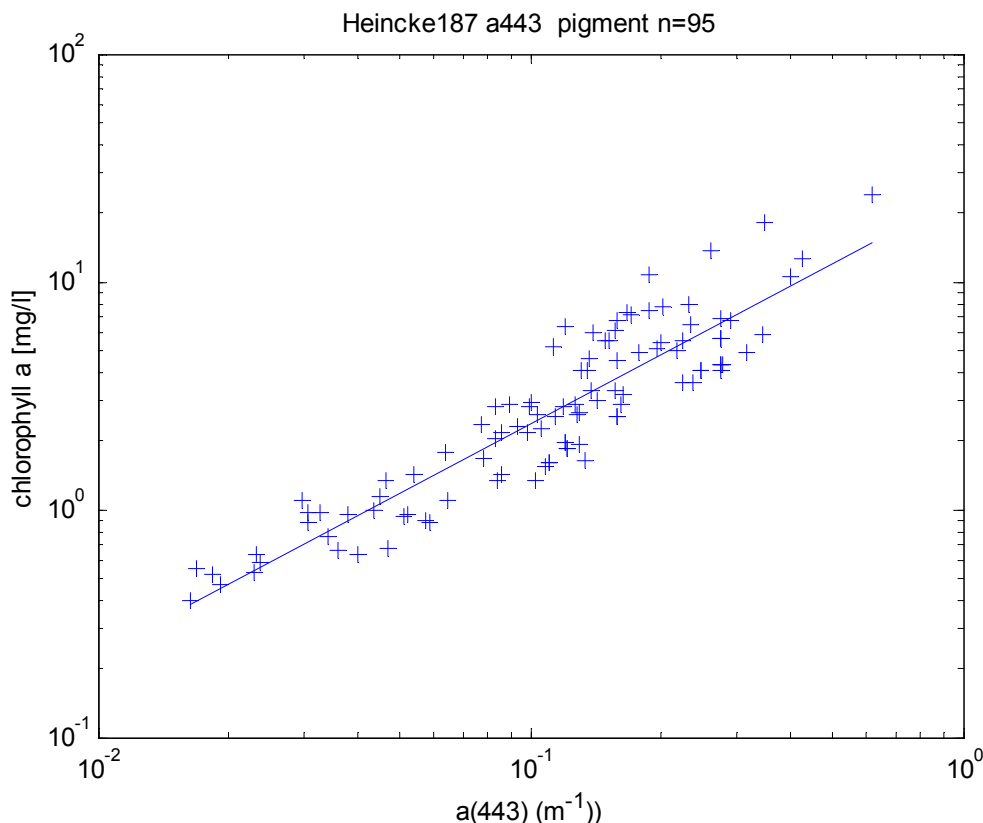


Fig. 5 Relationship between pigment absorption and chlorophyll *a* concentration for samples of the Southern North Sea., conversion equation is $\text{algal_2} = 21 * a_{\text{pig}}^{1.04}$

This relationship was confirmed by Sorensen et al. from measurements in the Skagerrak and northern North Sea along the Norwegian coast.

$$\text{Chl2.hp1c} = 21,848 \times a_{\text{pig}}^{1,044}$$

As mentioned above, the relationship between a_{pig} and the chlorophyll concentration is also valid for algal_1 :

$$\text{Algal_1} = 21 \cdot a_{\text{pig}}^{1.04}$$

but only when case 2 water pixels are excluded from this comparison (s. Fig. 6). This exclusion was done “by hand” to separate the two clusters. As it turned out, the upper cloud of Fig. 5 are mainly pixels from geographical regions with case 2 water. The regression line was then determined for the lower cloud.

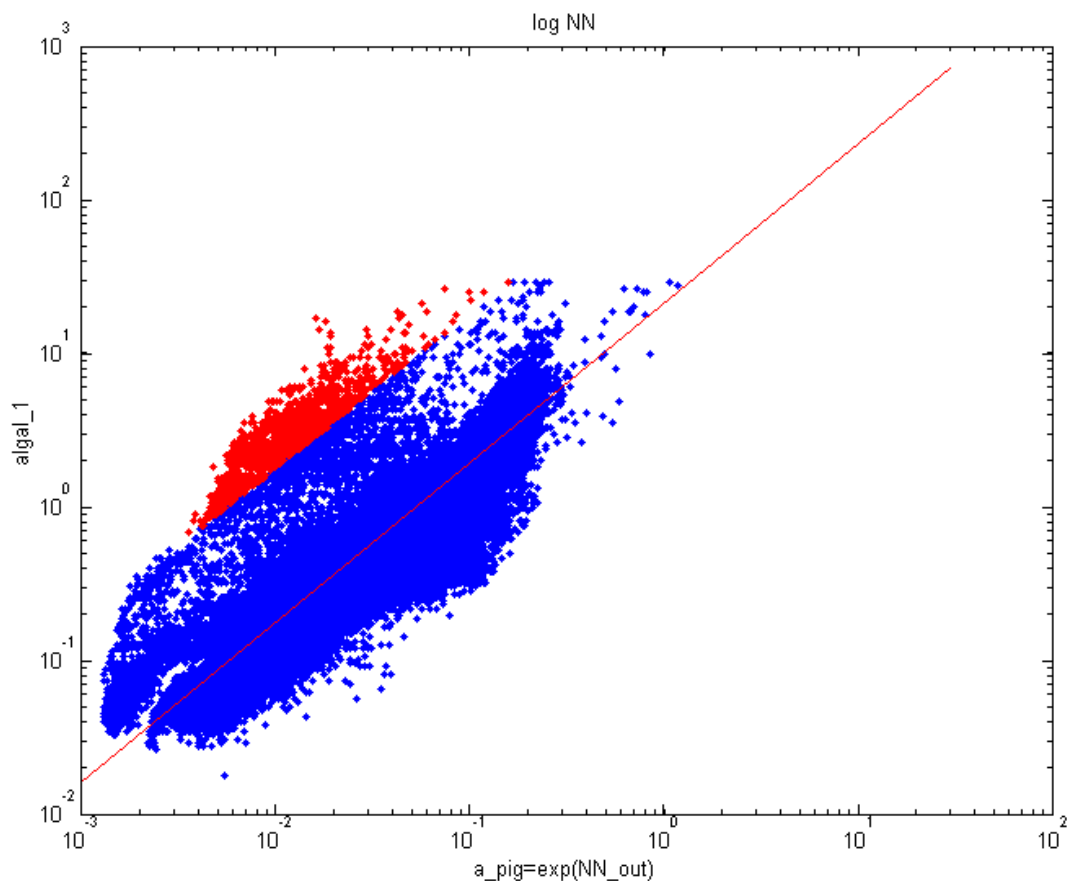


Fig. 6 Relationship between pigment_absorption (output of the NN) and algal_1 , the red dots indicate pixels at coastal case 2 water locations. The line shows the relationship $\text{algal_1} = 21.0 \cdot a_{\text{pig}}^{1.04}$.

For the conversion of b_{tsm} into concentration of TSM dry weight the following factor was derived from our measurements (s. Fig. 7), which is in agreement with the factor determined from the Coastlooc data set (Babin 2003).

$$\text{TSM} = 1.72 * b_{\text{tsm}}$$

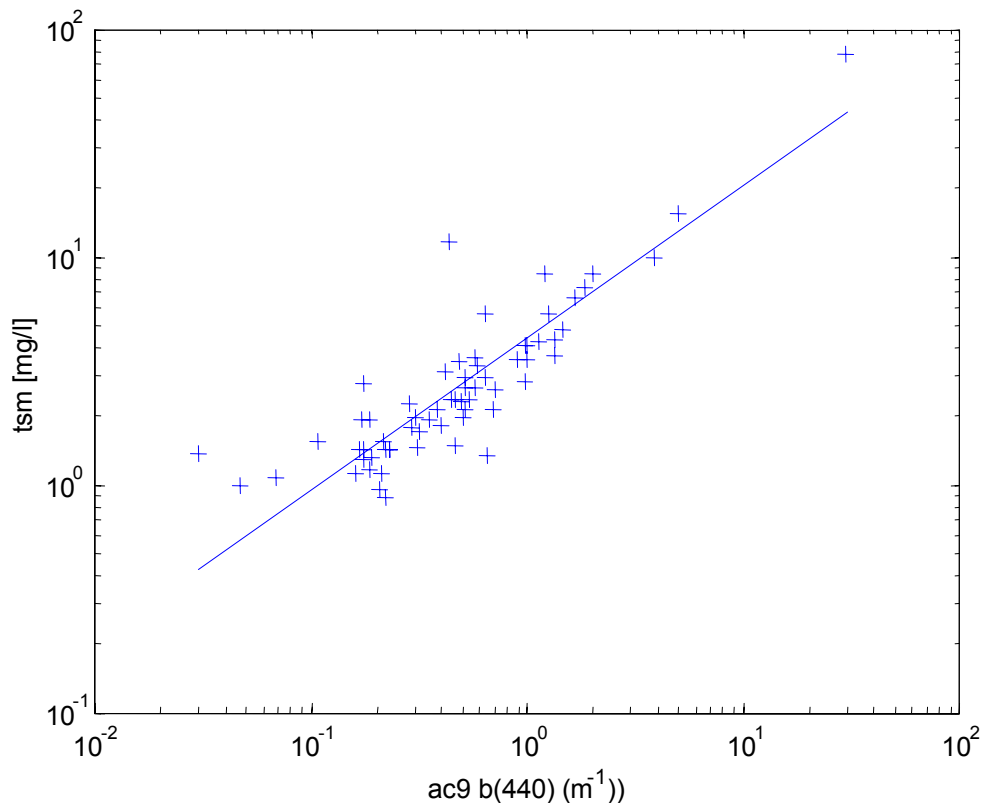


Fig. 7 Relationship between total particle scattering and total suspended matter (tsm) dry weight. Data of the Southern North Sea, cruise H187.

Calculation of the minimum irradiance attenuation coefficient k_{min} and the signal depth z_{90}

The downwelling irradiance attenuation coefficient k is computed for each MERIS band using the two-flow approximation $k = \sqrt{a_{\text{tot}}(a_{\text{tot}} + 2 * b_{\text{b_tot}})}$, with a_{tot} the total absorption coefficient, i.e. of water, pigments and yellow substance including bleached particles, and $b_{\text{b_tot}}$ is the backscattering coefficient of pure water and all particles in water. The backscattering coefficient is computed from the scattering coefficients. For water simply 0.5 of the scattering coefficient according to the Rayleigh phase function is used. For the particles we use a backscattering factor of 0.05, which is larger than the backscattering factor of 0.015 as determined from the phase function used in the model. Reason is that one has to take the shape factor into account, which we assume in the order of π .

The minimum attenuation coefficient k_{min} is then computed as the mean of the k values of those three bands with the smallest k values.

The signal depth z_{90} is then estimated simply as $1/k_{\min}$. It is given in negative numbers to produce a low (dark) grey level for water with a large signal depth and a bright grey level for waters with a small signal depth.

Validation of the algorithm enhancement

To test the new inversion scheme a BEAM processor was coded. The NN's used by this processor are the same as in the MERIS ground segment. Therefore all the validation results concerning the underlying (inverse) modelling apply for this processor too. It suffices here to prove that the retrieved values fit the model better than before.

For the test a subset of

MER_FR__2PNUPA20030806_100639_000000982018_00423_07491_0156.N1

in the German Bight was processed with the new processor. The frequency distribution of the quality indicator $q = (\mathbf{r}' - \mathbf{r})^2$ before and after the fit is shown in fig. 8. The improvement is obvious.

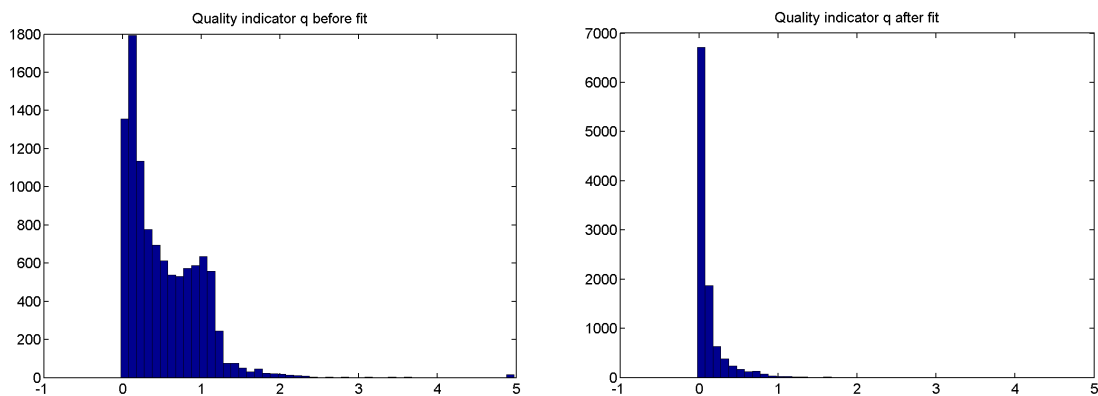


Fig. 8 Quality indicator before (left) and after (right) the optimization loop of the enhanced inversion scheme.

To illustrate the impact of the optimization in fig. 9 a measured reflectance spectrum is shown together with the spectrum corresponding to the first guess and the spectrum corresponding to the fit result, respectively.

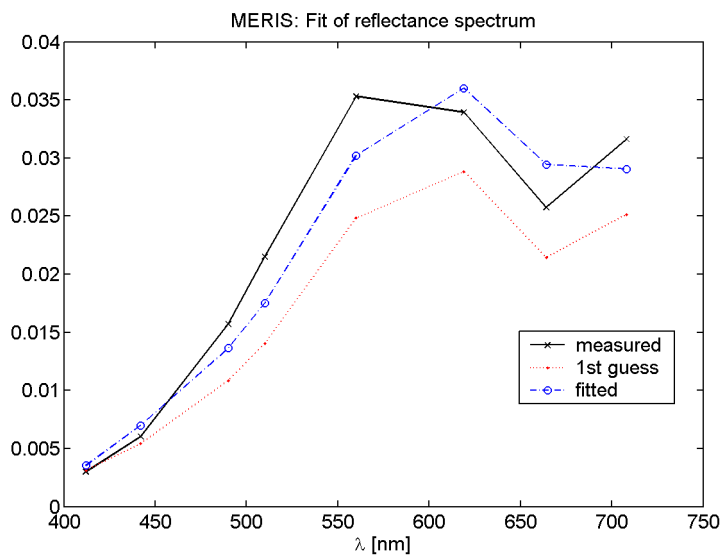



Fig. 9 Measured reflectance spectrum (black), spectrum corresponding to the first guess (red) and the spectrum corresponding to the fit result (blue).

References

- M. Babin, A. Morel, V. Fournier-Sicre, F. Fell and D. Stramski 2003, Light scattering properties of marine particles in coastal and open ocean waters as related to the particle mass concentration. *Limnol. Oceanogr.*, pp. 843–859
- R. Doerffer and H. Schiller, 2000, Neural Network for Retrieval of Concentrations of Water Constituents with the Possibility of Detecting Exceptional out of Scope Spectra. *Proc. IGARSS 2000*, pp. 714-717.
- C. D. Mobley, 1994, *Light and Water Radiative Transfer in Natural Waters*. Academic Press, Inc.
- A. Morel, 1974, Optical Properties of pure water and sea water. In *Optical aspects of oceanography*, ed. By N. G. Jerlov and Nielsen, E. S., pp 1-24, Academic New York.

	MERIS Case2 Regional	ATBD water Page 19 of 19
--	-----------------------------	-----------------------------

A. Morel and D. Antoine, 2000, ATBD 2.9: Pigment Index Retrieval in Case 1 Waters. ESA Doc. No. PO-TN-MEL-GS-0005, pp. 9-1 - 9-26; it can be downloaded from http://isat.esa.int/instruments/meris/pdf/atbd_2_09.pdf.

T. L. Petzold , 1972, Volume scattering functions for selected ocean waters. San Diego: Scripps Inst. Oceanogr., Ref 72-78, 79pp.

R. Pope and E. Fry, 1997, Absorption spectrum (380-700nm) of pure waters: II. Integrating cavity measurements, *Applied Optics*, pp 8710-8723.

H. Schiller and R. Doerffer, 1999, Neural Network for Emulation of an Inverse Model - Operational Derivation of Case II Water Properties from MERIS data. *Int. J. Remote Sensing*, vol. 20, pp. 1735-1746.

H. Schiller, 2000, Feedforward-Backpropagation Neural Net Program ffbp1.0. Report GKSS 2000/37, ISSN 0344-9626.

H. Schiller and R. Doerffer, 2005, Improved Determination of Coastal Water Constituent Concentrations from MERIS Data, *IEEE transactions on geoscience and remote sensing*, vol 43, pp. 1585-1591, 2005.

H. Siegel, M. Gerth, T. Ohde, T. Heene, 2005, Ocean colour remote sensing relevant water constituents and optical properties of the Baltic Sea. *Journal of Remote Sensing*, pp. 315-330.